Pharmaceutical Research, Vol. 23, No. 6, June 2006 (© 2006)
DOI: 10.1007/s11095-006-0165-1

Research Paper

Nontoxic Suramin as a Chemosensitizer in Patients: Dosing Nomogram Development

Danny Chen,[1] Sae Heum Song,[1] M. Guillaume Wientjes,[1,2,5] Teng Kuang Yeh,[1] Liang Zhao,[1] Miguel Villalona-Calero,[2,3] Gregory A. Otterson,[2,3] Rhonda Jensen,[1,2] Michael Grever,[2,3] Anthony J. Murgo,[4] and Jessie L-S. Au[1,2]

Received December 13, 2005; accepted January 31, 2006

Purpose. We reported that suramin produced chemosensitization at nontoxic doses. This benefit was lost at the ~10-fold higher, maximally tolerated doses (MTD). The aim of the current study was to identify in patients the chemosensitizing suramin dose that delivers 10–50 μM plasma concentrations over 48 h.
Methods. Nonsmall cell lung cancer patients were given suramin, paclitaxel, and carboplatin, every 3 weeks. The starting chemosensitizing suramin dose was estimated based on previous results on MTD suramin in patients, and adjusted by using real-time pharmacokinetic monitoring. A dosing nomogram was developed by using population-based pharmacokinetic analysis of phase I results (15 patients, 85 treatment cycles), and evaluated in phase II patients (19 females, 28 males, 196 treatment cycles).
Results. The chemosensitizing suramin dose showed a terminal half-life of 202 h and a total body clearance of 0.029 L h^{-1} m^{-2} (higher than the 0.013 L h^{-1} m^{-2} value for MTD of suramin). The dosing nomogram, incorporating body surface area as the major covariate of intersubject variability and the time elapsed since the previous dose (to account for the residual concentrations due to the slow elimination), delivered the target concentrations in >95% of treatments.
Conclusions. The present study identified and validated a dosing nomogram and schedule to deliver low and nontoxic suramin concentrations that produce chemosensitization in preclinical models.

KEY WORDS: chemosensitization; dosing nomogram; neoplasms; suramin.

INTRODUCTION

Our laboratory has shown acidic and basic fibroblast growth factors (aFGF and bFGF), expressed in solid tumors, as a cause of chemoresistance. The combined presence of these two proteins, at clinically relevant concentrations, induces an up to 10-fold resistance to drugs with diverse structures and action mechanisms, without altering drug accumulation. Inhibitors of aFGF and bFGF, including the respective monoclonal antibodies and suramin, reverse the FGF-induced resistance (1–3).

Suramin, an aromatic polysulfonated compound, has multiple, concentration-dependent effects. Targets inhibited by <50 μM suramin include reverse transcriptase, protein kinase C, transforming growth factor β, bFGF, and RNA polymerase, and targets affected by >50 μM suramin include interleukin-2, insulin-like growth factor I, topoisomerase II, epidermal growth factor, and tumor necrosis factor α (4–7). Suramin induces cell cycle arrest at the G1 phase at >50 μM (8–11), and shows appreciable cytotoxicity at >100 μM.

Suramin has been evaluated as an anticancer agent since the 1980s, and has shown activities in several malignancies, most notably in prostatic carcinoma (12,13). These earlier studies used maximally tolerated doses (MTD) yielding 100–200 μM suramin in plasma (equivalent to approximately 150–300 μg mL^{-1}) (13–15). The half-life of MTD suramin is unusually long (30–50 days), and results in significant drug accumulation upon repeated dosing. This pharmacokinetic property, together with its significant host toxicities, mandated the use of real-time pharmacokinetic analysis and adaptive control to calculate the suramin dose for individual patients. Subsequent findings of low interpatient variability in the suramin clearance and further population-based pharmacokinetic (PPK) analysis have led to the recommendation of using fixed dose schedules, consisting of series of infusions with sequentially decreasing doses or increasing intervals, to maintain plasma concentrations in the 70–200 μM range (16,17).

We reported that suramin, at a dose that delivers plasma concentration between 10 and 50 μM, significantly enhances the therapeutic efficacy of chemotherapy (doxorubicin, pacli-

[1] College of Pharmacy, The Ohio State University, 496 West 12th Avenue, Columbus, Ohio 43210, USA.
[2] James Cancer Hospital and Solove Research Institute, The Ohio State University, Columbus, Ohio, USA.
[3] Department of Internal Medicine, The Ohio State University, Columbus, Ohio, USA.
[4] National Cancer Institute, Bethesda, Maryland, USA.
[5] To whom correspondence should be addressed. (e-mail: wientjes.1@osu.edu)

taxel, docetaxel, mitomycin) against well-established subcutaneous or metastatic human xenograft tumors (breast, prostate, bladder) in immunodeficient mice, without enhancing the host toxicity (1–3,18,19). We further found that this chemosensitizing effect of suramin was diminished at higher doses/concentrations (20), presumably due to cell cycle perturbations. These findings, together with the limited clinical efficacy of MTD suramin in previous combination chemotherapy studies (13,21–23), highlight the importance of maintaining the suramin concentration within the 10–50 μM range.

The above considerations led to the initiation of several phase II clinical trials of using nontoxic suramin as a chemosensitizer (24). The goal of the present study, conducted in conjunction with the phase I/II trials in non small cell lung cancer (NSCLC), was to develop a method to identify the chemosensitizing suramin dose that delivers 10 and 50 μM plasma concentrations over the duration when the chemotherapy agents (paclitaxel and carboplatin) are present at therapeutically significant levels (i.e., 48 h). To accommodate the residual drug due to the unusually long half-life and the need to maintain the drug concentrations within the range that produces chemosensitization, we first used real-time pharmacokinetic studies to identify the suramin dose in the second or later cycles in the phase I study. This method was successful in maintaining desired suramin concentrations, but was labor-intensive and cannot be readily implemented in the community settings. Hence, we used population pharmacokinetic (PPK) analysis of the results in the first two cohorts of phase I patients to develop a dosing nomogram, which was then evaluated in an additional phase I cohort and subsequently in phase II patients.

MATERIALS AND METHODS

Patient Protocols and Treatments

Details on patient treatments had been described in a previous publication (24). The following provides the information pertinent to the present study. Briefly, a patient with pathologically or cytologically confirmed advanced (IIIB or IV) NSCLC received a 30-min infusion of suramin, followed immediately by a 3-h infusion of paclitaxel (starting at 175 mg m^{-2} and escalating to 200 mg m^{-2} after the suramin dose was established), and then a 1-h infusion of carboplatin [area under the plasma concentration–time curve (AUC) of 6 mg min mL^{-1}]. The phase I trial was open to all comers, whereas the phase II trial included two groups of patients (chemotherapy-naive or chemotherapy-refractory). For the present study, all patients with adequate samples for pharmacokinetic evaluation were included. The target suramin plasma concentration was initially set between 10 and 50 μM for 72 h and the initial dose, calculated based on the published clinical data for MTD suramin (24,25), was 240 mg m^{-2} given as a single dose. Based on the results in the first cohort of six patients, the target concentrations were amended to between 10 and 50 μM over 48 h, and suramin was administered as two split doses (two-thirds on the first day and one-third on the second day). The suramin dose for subsequent cycles (i.e., second and later cycles) was reduced to compensate for the residual plasma concentration at 72 h pretreatment. A total of 62 patients (15 in phase I and 47 in phase II) were studied for pharmacokinetics. Phase I patients received a total of 85 treatment cycles, with a median of 6 cycles. Phase II patients received a total of 198 treatment cycles, with a median of 4 cycles. All patients showed renal and hepatic function tests within the normal limits, before and after treatments.

Pharmacokinetic Studies and Data Analysis

Suramin or paclitaxel was extracted from plasma or urine, and analyzed with previously published high-performance liquid chromatography methods (26). The detection limit was 0.5 μg mL^{-1} for suramin and 15 ng mL^{-1} for paclitaxel. For carboplatin, plasma ultrafiltrates containing the free drug (not bound to plasma proteins) were obtained, diluted with deionized water, and analyzed for platinum content by using inductively coupled plasma mass spectrometry, as previously described (27).

To determine whether suramin affected the plasma protein binding of paclitaxel and vice versa, 2 mL human plasma containing nonradiolabeled paclitaxel and tritium-labeled suramin, or nonradiolabeled with tritium-labeled paclitaxel, was placed in the upper chamber of an ultrafiltration unit that was separated from the lower chamber by a cellulose membrane (molecular weight cutoff at 10,000; Amicon, Beverly, MA, USA). The unit was maintained in room temperature for 45 min, followed by centrifugation at 2,000 × *g* for 30 min. Aliquots (25 μl each) were removed from the top chamber prior to ultrafiltration (containing free plus bound drug), and from the bottom chamber after ultrafiltration (containing only the free drug), and analyzed for paclitaxel or suramin by using liquid scintillation counting. The extent of protein binding was calculated as (Total concentration − Free concentration) / (Total concentration).

Pharmacokinetic analysis was performed with WinNonlin. Phase I suramin plasma data were analyzed by using open two- and three-compartment linear models with a constant infusion input. For paclitaxel and carboplatin data and phase II suramin data, we used noncompartmental analysis. Renal clearance was calculated as the amount of suramin excreted in 24-h urine divided by the plasma AUC over the same 24-h period.

Overview of Development and Validation of Dosing Equations/Nomogram

Figure 1 outlines the schema. First, we used the pharmacokinetic results in the first cohort of six phase I patients to determine the duration that covered >90% of the paclitaxel/carboplatin AUC, with the goal of maintaining the plasma suramin concentrations at between 10 and 50 μM over this duration. This led to adjustments in the suramin regimen; administering suramin in two split doses yielded the target concentrations over 48 h in the second cohort of six patients. The pharmacokinetic results of these 12 patients were then used with PPK analysis to derive suramin dosing equations, which were then used to predict the dose in three additional phase I patients. Through retrospective and prospective analyses of the precision and accuracy of the PPK-based dosing equations, a correction factor was identified and used

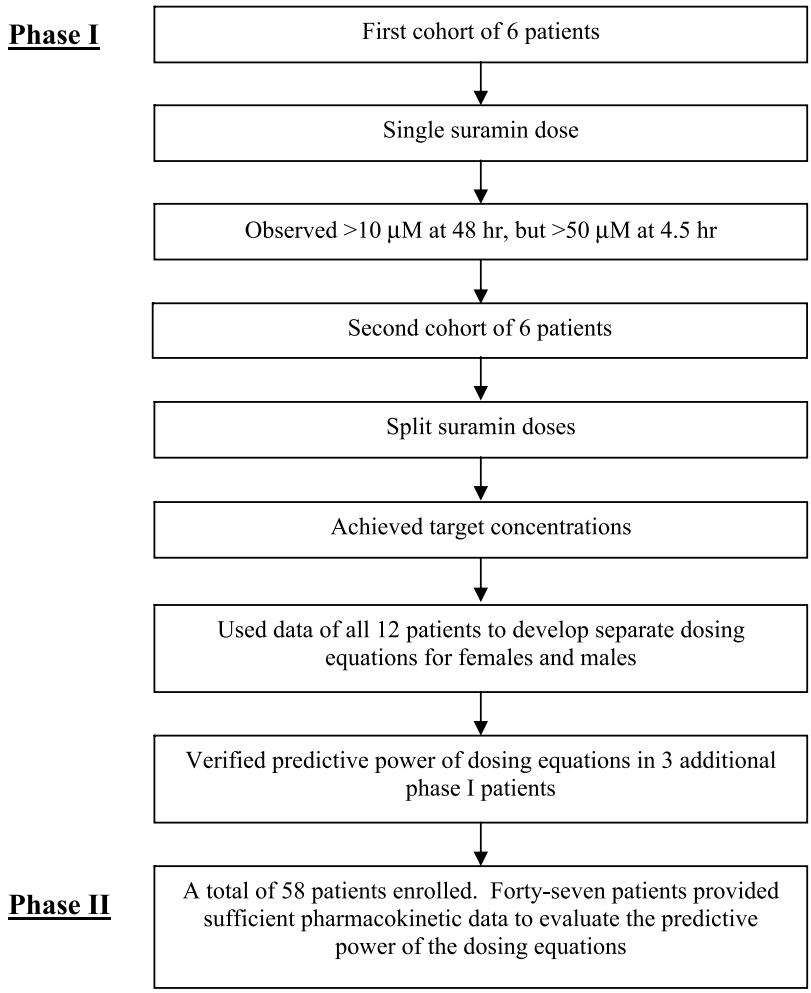

Fig. 1. Development and validation of dosing nomogram: Experimental Design.

to derive a dosing nomogram. The predictive power of the nomogram was evaluated in 47 phase II patients.

Population-Based Pharmacokinetic Analysis

Suramin data were analyzed with the nonlinear mixed-effects modeling approach (NONMEM Version V; UCSF, San Francisco, CA, USA). PPK analysis identifies the sources of interindividual variability in pharmacokinetic parameters and is performed in a stepwise manner (28,29), as follows.

The first step is to define the appropriate structural model for the pharmacokinetic parameters of interest. Because ~90% of the area under the suramin plasma concentration–time curve was accounted for by the area under one phase (i.e., terminal phase), we used a one-compartment model for PPK analysis due to its relative ease. Equation (1) describes the population-based plasma concentrations (C) as a function of clearance (CL) and volume of distribution (V), in a one-compartment model.

$$C_{ij} = \frac{\text{Dose}}{V_j} e^{-\left(\frac{CL_j}{V_j}\right) \times time_i} \quad (1)$$

where subscript i represents time and subscript j denotes a patient. For example, C_{ij} is the predicted plasma concentration at a particular time i for a patient j. The NONMEM subroutines describing this model are supplied as prewritten programming codes ADVAN1, TRAN2 in the PREDPP library of the NONMEM software.

In NONMEM analysis, error functions are used to describe the random deviations between model-predicted data and observed data, for individual pharmacokinetic parameters. Our objective was to identify the dose that can be calculated based on CL and V. Hence, the analysis focused on these two parameters. Equations (2) and (3) describe the deviation of CL (CL_j) and V (V_j) in an individual patient from the population or typical values ($CL_{\wedge typ}$ and $V_{\wedge typ}$).

$$CL_j = CL_{\wedge typ} \times (1 + \eta_{CL}) \quad (2)$$

$$V_j = V_{\wedge typ} \times (1 + \eta_V) \quad (3)$$

where η_{CL} and η_V representing the interindividual variation in CL and V are random values normally distributed around a mean of zero with a variance of ω^2.

Equation (4) describes the residual error between the predicted *vs.* the observed concentration; Y_{ij} is the observed plasma concentration of the jth individual at the ith sampling time, C_{ij} is the PPK Model-predicted values, and ε_{1ij} and ε_{2ij} are the proportional and additive errors, respectively, with a mean of zero and a variance of σ^2.

$$Y_{ij} = C_{ij} \times (1 + \varepsilon_{1ij}) + \varepsilon_{2ij} \quad (4)$$

Next, the physiological or pathological parameters of patients (referred to as covariates) that significantly contributed to the interindividual variability in CL and V were incorporated into the model (referred to as the Full Model). This was accomplished by examining the relationships between covariates and pharmacokinetic parameters in individual patients by using linear regression; covariates that showed a coefficient of determination (r^2) of greater than 0.4 with a 5% significance ($p < 0.05$) were selected as candidate covariates. A candidate covariate was incorporated into the model if its inclusion reduced the objective function value of the model by at least 3.9 (i.e., χ^2 value associated with $p < 0.05$ for 1 degree of freedom). To ascertain that the selected covariates played an important role in the model performance, the final model (referred to as PPK Model) was obtained by removing insignificant covariates from the Full Model in a more restrictive backward elimination process. In this process, a covariate was retained if its removal resulted in an increase in the objective function by at least 7.9 (χ^2 value associated with $p < 0.005$ and 1 degree of freedom).

Evaluation of Dosing Equations

The PPK Model (further described in Results), combined with individual patient parameters, yield PPK Model-based doses for each treatment cycle. The performance of the PPK Model-based dosing equations was evaluated as follows. First, we calculated the target dose (referred to as Ideal Dose) that would yield a plasma concentration of 15 μM suramin at 48 h ($C_{48\,h,target}$), using Eq. (5).

$$\text{Ideal Dose} = \frac{\text{administered dose} \times \left(C_{48h,target} - C_{pre} \times e^{-k\times 48}\right)}{\left(C_{48h,observed} - C_{pre} \times e^{-k\times 48}\right)} \quad (5)$$

where C_{pre} is observed predose suramin concentration and $C_{48h,observed}$ is the observed or fitted concentration at 48 h. The deviation of PPK Model-predicted dose from Ideal Dose for each cycle (Deviation) was calculated by using Eq. (6). The mean and standard deviation of Deviations of all cycles represent the accuracy and precision, respectively, of the PPK Model-predicted doses.

$$\text{Deviation from Ideal Dose} = \left(\frac{\text{Ideal Dose} - \text{Predicted dose}}{\text{Ideal Dose}} \times 100\%\right) \quad (6)$$

Similarly, the % deviations of the PPK Model-predicted plasma concentrations of each cycle was calculated by using Eq. (7), and the accuracy and precision of the PPK Model-predicted concentrations were calculated as described for the PPK Model-predicted doses.

$$\text{Deviation from target concentrations} = \left(\frac{(C_{predicted} - C_{observed})}{C_{predicted}} \times 100\%\right) \quad (7)$$

Validation of PPK Model-Based Dosing Method in Phase II Study

The final dosing equations and the resulting nomogram were adopted for the phase II study. A total of 58 patients were accrued to the phase II trial. The first 11 phase II patients provided only 0- and 24-h samples. We later amended the protocol and obtained additional samples (predose, 0.5, 3.5, 4.5, 6, 24, and 26 h) that enabled the determination of the 48-h concentration through pharmacokinetic data fitting (actual samples were not available). The performance of the dosing nomogram was evaluated by comparing the observed/fitted concentrations to the target range of 10–50 μM over 48 h.

Statistical Analysis

Statistical significance of the differences in pharmacokinetic parameters between groups was analyzed by using Student's *t* test. The Akaike Information Criterion and the Schwartz Criterion were used to compare the fitting of two- and three compartment pharmacokinetic models to the suramin plasma concentration–time data (30).

RESULTS

Pharmacokinetics of Paclitaxel and Carboplatin

The results show similar clearance and terminal half-lives for the two paclitaxel doses used (initially 175 mg kg^{-1}, escalating to 200 mg kg^{-1}). For carboplatin, the average dose was 679 ± 115 mg (range, 514–894; median, 654). The average AUC from time 0 to 48 h was 1.27 ± 0.24 mg min mL^{-1} for paclitaxel (200 mg kg^{-1} dose) and 6.3 ± 1.4 mg min mL^{-1} for carboplatin, and the respective AUC from time 0 to time infinity were 1.33 ± 0.27 and 6.4 ± 1.4 mg min mL^{-1}, indicating the attainment of >92% and >99% of the total AUC during the first 48 h. A comparison of the paclitaxel and carboplatin pharmacokinetics in the present trial with literature data (31–34) showed no significant changes due to the addition of suramin (not shown).

Pharmacokinetics of Chemosensitizing Suramin

The target suramin concentration range was initially set at 10–50 μM over 72 h. Results in the first six patients indicated the attainment of the target concentration of 10–20 μM at 72 h in five patients, but showed peak levels exceeding 50 μM in all patients. As >90% of the AUCs of paclitaxel and carboplatin were attained in the first 48 h, the target suramin concentrations were amended to between 10

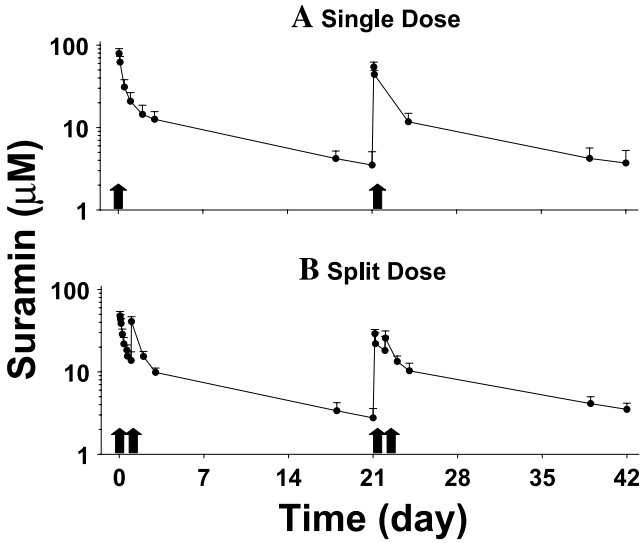

Fig. 2. Suramin plasma concentration–time profiles. Suramin was given by single doses (panel A, total of 19 treatments) or by split doses (panel B, total of 66 treatments). Arrows indicate times for the initiation of 30-min suramin infusion. Data are mean + 1 SD. Data points are connected by straight lines.

and 50 μM over 48 h. We calculated that these concentrations could be achieved by giving suramin in two split doses, with two-thirds given on the first day and the remaining one-third given 24 h later (Fig. 2). This schedule yielded the target concentration range of <50 μM immediately after the 3-h paclitaxel infusion and >10 μM at 48 h, in all of the subsequent 66 treatments administered to 13 patients (including the remaining treatments in four of the original first six patients and nine additional patients).

The suramin dose was 240 mg m^{-2} for the first cycle and 146 ± 21 mg m^{-2} for the second and later cycles. Figure 2 shows the plasma concentration–time profiles. Analysis of the data of the first cycle by using two- and three-compartment body models showed no significant difference in the goodness-of-fit ($p = 0.5$ by the Akaike Information Criterion and $p = 0.7$ by the Schwartz Criterion) and yielded nearly identical total body clearance (<10% difference, $p > 0.4$). The pretreatment suramin concentrations during the second through tenth treatment cycles remained relatively constant at about 4 μg mL^{-1} (range, 2.95–4.80 μg mL^{-1}). As the doses for these cycles were calculated by using real-time pharmacokinetics based on the parameters in individual patients (obtained by analyzing the data in the first cycle), the nearly constant pretreatment concentrations for up to 30 weeks of treatment indicate no changes in drug disposition over time.

Table I summarizes the pharmacokinetic parameters of suramin in phase I patients. The renal clearance of suramin was determined in 38 phase II patients; 1.21 ± 1.05% of the dose was excreted as unchanged drug in 24 h and the calculated renal clearance was 2.05 ± 1.69 mL h^{-1} m^{-2} (range, 0.18–8.7 mL h^{-1} m^{-1}, equal to 7.09 ± 5.76% of the total plasma clearance). The renal clearance did not show a significant correlation with the creatinine clearance ($r = 0.123$, $p = 0.46$).

In Vitro Protein Binding of Paclitaxel and Suramin

The plasma protein binding of suramin at clinically achievable concentrations (i.e., 10 and 100 μg mL^{-1}) remained constant at 99.6 ± 0.02% ($n = 3$), and was not altered by the addition of 10 μg mL^{-1} paclitaxel. The plasma protein binding of paclitaxel was 90.8 ± 0.5%, 90.8 ± 0.2%, and 88.9 ± 0.3% ($n = 3$ each) at clinically achievable concentrations of 0.1, 1, and 10 μg mL^{-1}, respectively. Addition of 100 μg mL^{-1} suramin did not affect the binding of paclitaxel at 0.1 and 1 μg mL^{-1} concentration, but significantly, albeit only slightly, decreased the paclitaxel binding at 10 μg mL^{-1}, from 88.9% to 88.3 ± 0.2%. This corresponded to a 5% increase in the free fraction of paclitaxel at 10 μg mL^{-1} (i.e., from 11.1% to 11.7%). This relative small interaction between the two drugs did not affect the disposition of paclitaxel, as in the present study its pharmacokinetics is not significantly different from previous studies where it was given only with carboplatin (35–37).

PPK-Based Pharmacokinetic Analysis

Plasma concentration–time profiles of 53 cycles obtained in the first 12 patients were analyzed by using PPK, to develop easy-to-use dosing equations. We reasoned that this task could be accomplished by using the simplest pharmacokinetic model, capable of reliably described plasma concentrations between 48 h (needed to assess maintenance of target concentrations) and the start of the next treatment cycle (determinant of the next dose). The dominance of the terminal phase (β phase half-life was 40 times the α-phase half-life, and ~90% of the total AUC was accounted for by the area under the terminal phase, calculated as B/β) led to the selection of a monoexponential model for PPK.

Table I. Pharmacokinetic Parameters of Suramin

Pharmacokinetic parameters	Literature (33)	Present study
Dose (mg m^{-2})	>2,000	240
AUC (μg h mL^{-1})	NA	8.37 ± 1.89
Alpha half-life (h)	14.8 ± 7.5	5.12 ± 1.54[b]
Beta half-life (day)	41 ± 23	8.61 ± 2.28[b]
V_1 (L m^{-2})	3.0 ± 0.6	1.94 ± 0.26[b]
V_2 (L m^{-2})	10.6 ± 3.1	6.50 ± 1.82[b]
V_{dss} (L m^{-2})	13.6 ± 3.2[a]	8.45 ± 1.88[b]
CL (L h^{-1} m^{-2})	0.013 ± 0.006	0.029 ± 0.006[b]

Results of suramin used as a chemosensitizer at low dose in 15 patients are compared to literature data obtained during Near-MTD application as a cytotoxic agent (33). As the pharmacokinetics of low dose suramin (cycle 1) was best described by a two-compartment model, this data is presented, and compared to a two-compartment analysis of high dose suramin. High dose suramin is adequately described by either a two- or a three-compartment model (33). Because the current study administered suramin every 3 weeks, whereas earlier studies administered suramin at more frequent intervals, the dose and AUC were normalized per 3-week interval. Mean ± standard deviation. NA, not available.

[a] V_{dss} was estimated as the sum of V_1 and V_2; standard deviation was calculated according to the error propagation rule $(SD1^2 + SD2^2)^{1/2}$.

[b] $p < 0.05$, unpaired two-tailed Student's t test compared to literature.

Table II. Relationship Between Suramin Clearance and Volume of Distribution and Clinical Parameters

	CL ($L\ h^{-1}$)	V (L)	Weight (kg)	IBW[a] (kg)	Height (in.)	BSA (m^2)	Age (years)	Gender	CrCL ($mL\ min^{-1}$)	Serum creatinine ($mg\ dL^{-1}$)	Serum albumin ($g\ dL^{-1}$)
						Numerical values					
Mean	50.4	18.2	79.3	68.5	68.5	1.94	60.1	8 male	88.2	0.94	4.22
SD	±11.7	±3.2	±11.1	±9.1	±3.3	±0.17	±9.2	2 female	±18.8	±0.13	±0.37
						Correlation with CL or V					
CL: *r*	1	0.577	0.789	0.710	0.632	0.789	0.569	−0.904	0.423	0.286	−0.332
CL: *p*	NA	(0.081)	(0.007)	(0.021)	(0.050)	(0.007)	(0.086)	(0.000)	(0.224)	(0.423)	(0.348)
V: *r*	0.577	1	0.854	0.511	0.498	0.773	0.117	−0.477	0.641	0.181	−0.058
V: *p*	(0.081)	NA	(0.002)	(0.131)	(0.143)	(0.009)	(0.748)	(0.164)	(0.046)	(0.618)	(0.873)

Data were taken from all cycles of 10 of the first 12 phase I patients. Two patients with samples collected for <1 terminal suramin half-life were not included. Ideal body weight (IBW) was calculated as the sum of (50 for males and 45.5 for females) and (2.3 × (height in inches − 60)). Creatinine CL was calculated using the Cockroft-Gault equation. The correlation coefficients (r) of CL and V with gender were obtained by assigning arbitrary values of 1 for male and 2 for female patients. The p values for the correlations are also indicated.

Nine potential covariates [i.e., age, body weight, ideal body weight, height, body surface area (BSA) age, gender creatinine CL, creatinine concentration, and albumin concentration] were examined. Their values and correlation coefficients with CL and V are shown in Table II. The covariates that showed statistically significant correlations with CL were body weight and BSA. In these 12 patients, the CL was significantly higher in nine male than in the three female patients. Accordingly, gender was included as a covariate. Creatinine CL showed a significant correlation by the nonparametric Spearman correlation ($r = 0.636$, $p = 0.048$). The remaining covariates did not show significant correlations in the linear regression analysis, and were not further evaluated. As body weight and BSA are strongly correlated ($r = 0.97$, $p < 0.001$), and as BSA is more widely used in dose determinations for oncology patients, only BSA (but not body weight) was used in the Full Model for $CL_{\wedge typ}$ [Eq. (8)]. V showed a significant correlation with BSA. Further testing showed improved model performance when BSA^2 was used as covariate instead of BSA. No other covariates reached statistical significance. The Full Model for $V_{\wedge typ}$ is described by Eq. (9).

$$CL_{\wedge typ} = (\theta_1 \times BSA + \theta_2 \times CrCL + \theta_3) \times (1 - \theta_4) \quad (8)$$

$$V_{\wedge typ} = \theta_5 \times BSA^2 + \theta_6 \quad (9)$$

where θ_1 and θ_2 describe the effects of BSA and CrCL on $CL_{\wedge typ}$, respectively. For males, θ_4 was set to zero. For females, θ_4 represents the difference between the clearance values for males and females. θ_5 is the proportionality constant that describes the effect of (BSA^2) on $V_{\wedge typ}$. θ_3 and θ_6 reflect the intercept values for CL and V, with the effects of the covariates removed.

Full Model was subsequently simplified by eliminating the covariates that did not significantly affect the model performance. Results are summarized in Table III. Removal of the fixed-effect parameters, θ_2, θ_3, and θ_6, from the Full Model altered the objective function value by less than 7.9,

Table III. Estimates for Population Model Parameters

	Full model				Population model				
			95% Confidence interval				95% Confidence interval		Difference in minimum values of objective function
Parameters	Mean	CV%	Low	High	Mean	CV%	Low	High	
θ_1 ($L\ h^{-1}\ m^{-2}$)	9.40	190	−1.97	20.8	26.2	2.70	24.6	27.4	15.47
θ_2	0.10	137	0.04	0.19	NA	NA	NA	NA	6.03
θ_3 ($L\ h^{-1}$)	24.8	106	8.09	41.5	NA	NA	NA	NA	2.59
θ_4	0.39	20	0.34	0.44	0.31	13.1	0.28	0.34	41.57
θ_5 ($L\ m^{-4}$)	4.30	24	3.62	4.92	5.13	4.40	4.49	5.57	29.47
θ_6 (L)	1.50	229	−0.72	3.90	NA	NA	NA	NA	1.84
$k_{\wedge typ}$ (h^{-1}, male)	NA	NA	NA	NA	0.0026	7.3	0.0023	0.0030	NA
$k_{\wedge typ}$, (h^{-1}, female)	NA	NA	NA	NA	0.0022	4.7	0.0020	0.0024	dNA

The population pharmacokinetic parameters were obtained using data from the first 12 patients (54 treatment cycles) in the phase I study. Fitted values for different fixed effect parameters [θ_1–θ_6 of Eqs. (8) and (9)] and estimates of variability of the estimates are presented. θ_2, θ_3, and θ_6 were removed from the final population model since their removal increased the objective function value by less than 7.9. NA: not applicable.

which is the value required for inclusion (29). Removal of these three parameters simultaneously altered the objective function value by 7.26. Removal of θ_2 rendered the model equations independent of the creatinine CL and simplified the model. The remaining three significant parameters were θ_1, θ_4, and θ_5. The final PPK Model is described by Eqs. (10) and (11).

$$CL_{\wedge typ} = (\theta_1 \times BSA) \times (1 - \theta_4) \quad (10)$$

$$V_{\wedge typ} = \theta_5 \times BSA^2 \quad (11)$$

Table III shows the parameter estimates and their coefficient of variations (CV) and 95% confidence intervals. The resulting final PPK Model, using only the two covariates BSA and gender, reduced the estimated interindividual variability in CL by 5-fold (from 30% to 6%) and the variability in V by 6-fold (from 20% to 3%).

Derivation of PPK Model-Based Dosing Equations

Due to the residual suramin concentration at the time of the second and later treatment cycles, separate equations are required to calculate the doses for the first treatment cycle and subsequent cycles.

The first dose was calculated by using Eq. (12), a simplified version of Eq. (1).

$$\text{Dose} = \frac{C \times V}{e^{-k \times t}} \quad (12)$$

Hence, dose calculation requires the values of V and k, the elimination rate constant. Equation (13) describes $k_{\wedge typ}$, as a function of $CL_{\wedge typ}$ and $V_{\wedge typ}$.

$$k_{\wedge typ} = \frac{CL_{\wedge typ}}{V_{\wedge typ}} \quad (13)$$

The value of k for each patient was calculated by using Eqs. (10), (11), and (13). The average k value ($k_{\wedge typ}$) was 0.0026 h^{-1} for males and 0.0022 h^{-1} for females. $k_{\wedge typ}$ showed a low variability within the same gender (CV of 7% for males and 5% for females). Substituting the values of $k_{\wedge typ}$ for each gender and the desired C of 15 μM or 21.4 μg mL^{-1} at 48 h into Eq. (12) yielded Eq. (14).

$$\begin{aligned}\text{First cycle dose (mg)} &= \frac{(21.4 \times 5.13 \times BSA^2)}{e^{-(0.0026 \text{ or } 0.0022 \times 48)}} \\ &= \text{FACTOR1} \times BSA^2\end{aligned} \quad (14)$$

The numerical values of FACTOR1 were calculated to be 124 mg m^{-4} for males and 122 mg m^{-4} for females. For ease of dose calculation in later studies, the value of FACTOR1 was set at 125 mg m^{-4} for both genders.

To attain the same target concentrations of 21.4 μg mL^{-1} at 48 h during subsequent treatment cycles, the dose administered should replace the fraction of the dose that was eliminated during the interval between treatments. This is described in Eq. (15).

$$\begin{aligned}\text{Subsequent cycle dose (mg)} &= \text{First dose} \times \left(1 - e^{-k \times t}\right) \\ &= \text{FACTOR1} \times BSA^2 \times \left(1 - e^{-k \times t}\right)\end{aligned} \quad (15)$$

Note that in contrast to the first cycle, where t = 48 h, the value of t during subsequent cycles is a variable that equals the time lapsed since the previous cycle. Furthermore, the value of t for the first cycle was relatively short (i.e., 48 h), which resulted in a <2% difference in the FACTOR values for males and females. Because of this small difference, it was not necessary to adjust for the gender-related differences in the calculation of the first cycle doses (i.e., FACTOR1 was set at 125). On the other hand, calculations of doses for subsequent cycles with time intervals of approximately 3 weeks (i.e., $t \geq 504$ h) yielded ~9% higher values for males than for females, and gender-based dose adjustments were made.

PPK Model-Based Dosing Method: Precision and Accuracy Determination, and Refinement using Phase I Results

The precision and accuracy of the PPK Model was determined by retroactive analysis of the data of the first 12 phase I patients. The precision of plasma concentration prediction by PPK Model, evaluated by using Eq. (7), was 22%. A comparison of PPK Model-predicted dose and Ideal Dose [calculated by using Eq. (5) to yield a plasma concentration of 15 μM at 48 h) indicated a 13% overestimation in the model prediction. Equation (15) was therefore further modified by multiplying FACTOR1 with 0.88 (i.e., 1 divided by 1.13), to yield Eq. (16). The overestimation is likely a result of a slight overestimation of $V_{\wedge typ}$ and consequently the calculated dose.

$$\begin{aligned}\text{Subsequent cycle dose} = 0.88 \times \text{FACTOR1} \times BSA^2 \\ \times \left(1 - e^{-k \times t}\right)\end{aligned} \quad (16)$$

This refinement yielded an accuracy of 102 (range, 51–151; median, 100; 23% standard deviation) for individual treatment cycles in individual patients, and 100 (range, 74–121; median, 97; 13% standard deviation) for all treatments in all patients. Figure 3 shows the correlation between Refined PPK Model-predicted dose and Ideal Dose.

We next performed prospective analysis by using Eqs. (14) and (16) to calculate the suramin doses during the first and subsequent cycles, respectively, for three additional phase I patients. To maintain the peak suramin concentration below 50 μM, the suramin dose was administered in two parts with two-thirds of the total dose administered prior to chemotherapy, followed by the remaining one-third of the dose given 24 h after the first dose. The plasma concentrations in all treatments in these three additional phase I patients were within the target range of 10–50 μM over the 48-h duration. The difference between the observed and target plasma concentrations of 15 μM at 48 h were <17%. Based on the above results, the Refined PPK Model-based

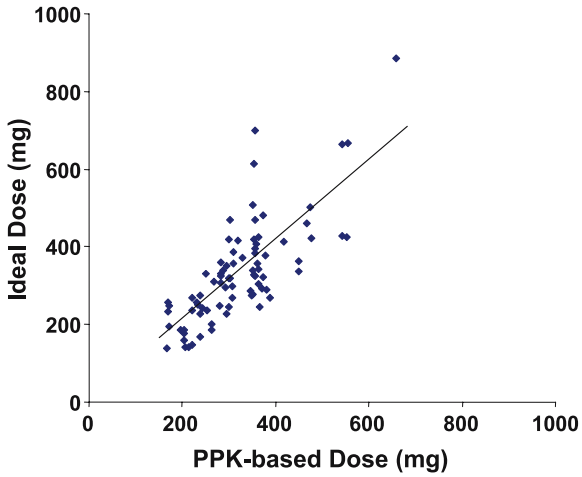

Fig. 3. Comparison of doses calculated by the PPK-based dosing method to Ideal Dose in individual patients. The first 12 patients in the phase I trial received suramin doses determined by real-time pharmacokinetics. For these patients, the Ideal Dose (mg m^{-2}) needed to obtain a plasma concentration of 15 μM at 48 h was calculated for each cycle as discussed in Materials and Methods. Diamonds represent data points and the line represents the linear regression line ($y = 1.04x$, $r^2 = 0.59$, $p < 0.0001$).

dosing equations [Eqs. (14) and (16)] were adopted and their performances were further evaluated in the subsequent phase II trial.

Validation of Refined PPK Model-Based Dosing Method in Phase II Patients

Forty-seven patients (receiving a total of 199 treatments) provided sufficiently detailed pharmacokinetic data for model validation. The suramin doses ranged from 135 to 673 mg. The target concentration range was successfully reached in >94% of administrations; suramin concentrations were below 50 μM in 194 of 199 cycles (97%) at the end of paclitaxel infusion (i.e., 4.5 h) and were at or above 10 μM at 48 h in 192 of 199 cycles (96%).

As the gender difference in suramin clearance observed in the phase I study was based on only five female patients, we extended the evaluation of the gender effect by comparing the suramin concentrations in male ($n = 28$) and female ($n = 19$) phase II patients. Note that the phase II female patients received on average 9% lower BSA-normalized doses. The results indicate no significant gender-related difference in suramin clearance (0.023 ± 0.006 L h^{-1} m^{-2} in females and 0.024 ± 0.005 L h^{-1} m^{-2} in males, $p > 0.37$).

DISCUSSION

Dose-Dependent Pharmacokinetics of Suramin

The current study showed that the dose of suramin used as a chemosensitizer is approximately 10% of MTD (38). A comparison of the pharmacokinetics of chemosensitizer suramin to the literature data on MTD suramin (38) shows a 2.5-fold higher clearance (Table I). This confirms the nonlinear suramin disposition suggested by a preliminary report on six subjects where the clearance of a 200-mg test doses was at least 2-fold lower than the clearance during MTD treatment with initial weekly administration of 2,000–2,800 mg m^{-2} [bar graph in (39)].

The processes for suramin clearance are not well understood. A study in patients with acquired immunodeficiency syndrome showed that suramin is essentially unmetabolized (40). The suggestion that renal clearance may play an important role was based on the finding that renal clearance accounted for total clearance in a single patient and the reduced total clearance in patients who received furosemide, a known inhibitor of tubular secretion (41). The present study provided an opportunity to test this hypothesized elimination; the results showed that renal clearance accounted for less than 10% of total clearance, which is in line with the value of ~20% we estimated from the published data on MTD suramin (42). The minor role of renal clearance for chemosensitizer suramin is also consistent with the exclusion of creatinine clearance as an important covariate of the PPK Model.

Several findings suggest dose-dependent tissue distribution of suramin. First, the plasma pharmacokinetics of MTD suramin was better described by a three-compartment open linear model than by a two-compartment model; the latter underestimated the plasma concentrations during the wash-

Table IV. PPK-Based Nomogram of Suramin

Suramin dose (mg) = FACTOR × BSA^2	
	FACTOR (mg/m^{-4})
Cycle 1	125
Subsequent cycles: Values of FACTOR depends on the elapsed time (days)	
Days since the administration of the first dose during previous cycle	FACTOR (mg/m^{-4})
21	80
22	82
23	84
24	86
25	87
26	88
27	90
28	91
29	92
30	93
31	94
32	95
33	96
34	97
35	98
36	98
37	99
38	100
39	100
41	102
42	102
44	103
47	104
49	105
52	106
55	106

out phase of a 12-week treatment (14,38). The existence of a slowly accumulating third compartment for MTD suramin is further supported by the slow tissue accumulation kinetics in rats receiving similar doses (43). In contrast, chemosensitizer suramin was well described by a two-compartment model. Second, chemosensitizer suramin showed a 40% smaller steady-state distribution volume. Third, progressive increases in the terminal half-life, which would be expected for significant drug accumulation in a deep, slowly equilibrating third compartment over time, was not observed during cycle 2 to cycle 10 (over 30 weeks). These findings suggest a deep compartment that is apparent only at MTD. Further studies to investigate the mechanisms of this unusual dose-dependent drug distribution and whether it contributes to the loss of the chemosensitization effect are warranted.

PPK Model-Based Dosing Nomogram

The present study used a one-compartment PPK Model (as opposed to using a two-compartment model). This approach eliminates the need of multiexponential equations and enables the derivation of an easy-to-use equation for clinical practice. The good predictive power of this equation was demonstrated in 50 patients (3 for phase I and 47 for phase II). The gender difference (14% lower clearance for 5 female patients) observed during the phase I trial led to the first dosing equations with gender-specific dose calculations. But because this difference was not observed in subsequent phase II studies in a larger group of female patients ($n = 19$), we recommend using a single dose calculation for both genders. To further facilitate clinical application, we constructed a nomogram that reduces the dosage calculation to a multiplication of the squared value of BSA with a tabulated factor to accommodate variations in treatment intervals (Table IV).

This study further showed that maintenance of patient plasma concentrations in the range of 10–50 μM for 48 h cannot be accomplished by a single intravenous short infusion starting at the beginning of the 48-h period. High peak concentrations can be avoided by using a number of approaches. In the current study, a split-dose schedule was successfully used to maintain concentrations within the desired range. An alternative approach, currently used in other phase II trials, is to administer an initial loading suramin dose, during the first treatment cycle, several hours earlier before chemotherapy.

The PPK Model-based dosing method for chemosensitizer suramin differs in several ways from the previously published fixed-dose method for MTD suramin (16,17). First, the suramin dose in earlier studies is targeted to continuously maintain plasma concentration between 100 and 200 μM, and results in a >10-fold higher dose requirement over 3 weeks compared to chemosensitizer dose used in the present study. Second, to maintain high and cytotoxic concentrations, MTD suramin regimen includes a loading dose followed by tapered follow-up doses at intervals increasing from 1 to 10 days and, in later studies, to >40 days. These types of fixed-dose schedules are not applicable for chemosensitizer suramin, where the emphasis is not on maintaining near-constant maximally tolerated concentrations, but rather on keeping plasma concentrations within the effective range (10–50 μM) for the duration when the chemotherapeutic agents are present at therapeutically significant values (e.g., 48 h for paclitaxel and carboplatin).

CONCLUSION

The present study provided a PPK Model-based nomogram to identify the chemosensitizer suramin dose in patients, to deliver the target plasma concentrations that produced chemosensitization in human xenograft models (1–3), over 48 h. This approach further eliminates the requirement of blood sampling for pharmacokinetic evaluation to guide dose adjustments. Our results further indicate nonlinear disposition of suramin in patients, and no significant pharmacokinetic interaction among suramin, paclitaxel, and carboplatin.

ACKNOWLEDGMENTS

This study was supported in part by R37CA49816, R01CA78577, R21CA91547 and U01CA76576 from the National Cancer Institute, NIH, DHHS. Patients were treated at a General Clinical Research Center (GCRC), which is supported by M01-RR00034 from the National Institutes of Health, DHHS. Analysis of carboplatin concentrations was performed by the Pharmacoanalytical Core Laboratory of The Ohio State University Comprehensive Cancer Center. Tong Shen's invaluable help in the renal clearance studies and management of clinical trial data is gratefully acknowledged.

REFERENCES

1. S. Song, M. G. Wientjes, Y. Gan, and J. L. Au. Fibroblast growth factors: an epigenetic mechanism of broad spectrum resistance to anticancer drugs. *Proc. Natl. Acad. Sci. USA* **97**:8658–8663 (2000).
2. S. Song, M. G. Wientjes, C. Walsh, and J. L. Au. Nontoxic doses of suramin enhance activity of paclitaxel against lung metastases. *Cancer Res.* **61**:6145–6150 (2001).
3. Y. Zhang, S. Song, F. Yang, J. L. Au, and M. G. Wientjes. Nontoxic doses of suramin enhance activity of doxorubicin in prostate tumors. *J. Pharmacol. Exp. Ther.* **299**:426–433 (2001).
4. C. E. Hensey, D. Boscoboinik, and A. Azzi. Suramin, an anticancer drug, inhibits protein kinase C and induces differentiation in neuroblastoma cell clone NB2A. *FEBS Lett.* **258**:156–158 (1989).
5. T. P. Wade, A. Kasid, C. A. Stein, R. V. LaRocca, E. R. Sargent, L. G. Gomella, C. E. Myers, and W. M. Linehan. Suramin interference with transforming growth factor-beta inhibition of human renal cell carcinoma in culture. *J. Surg. Res.* **53**:195–198 (1992).
6. E. De Clercq. Suramin: a potent inhibitor of the reverse transcriptase of RNA tumor viruses. *Cancer Lett.* **8**:9–22 (1979).
7. H. Nakane, J. Balzarini, E. De Clercq, and K. Ono. Differential inhibition of various deoxyribonucleic acid polymerases by Evans blue and aurintricarboxylic acid. *Eur. J. Biochem.* **177**: 91–96 (1988).
8. S. T. Palayoor, E. A. Bump, B. A. Teicher, and C. N. Coleman. Apoptosis and clonogenic cell death in PC3 human prostate cancer cells after treatment with gamma radiation and suramin. *Radiat. Res.* **148**:105–114 (1997).
9. L. Qiao, J. G. Pizzolo, and M. R. Melamed. Effects of suramin on expression of proliferation associated nuclear antigens in DU-145 carcinoma cells. *Biochem. Biophys. Res. Commun.* **201**: 581–588 (1994).

10. W. K. Evans, C. C. Earle, D. J. Stewart, S. Dahrouge, E. Tomiak, G. Goss, D. Logan, R. Goel, S. Z. Gertler, and H. Dulude. Phase II study of a one hour paclitaxel infusion in combination with carboplatin for advanced non-small cell lung cancer. *Lung Cancer* **18**:83–94 (1997).
11. J. H. Kim, E. R. Sherwood, D. M. Sutkowski, C. Lee, and J. M. Kozlowski. Inhibition of prostatic tumor cell proliferation by suramin: alterations in TGF alpha-mediated autocrine growth regulation and cell cycle distribution. *J. Urol.* **146**:171–176 (1991).
12. F. Hawking. Suramin: with special reference to onchocerciasis. *Adv. Pharmacol. Chemother.* **15**:289–322 (1978).
13. S. M. Tu, L. C. Pagliaro, M. E. Banks, R. J. Amato, R. E. Millikan, N. A. Bugazia, T. Madden, R. A. Newman, and C. J. Logothetis. Phase I study of suramin combined with doxorubicin in the treatment of androgen-independent prostate cancer. *Clin. Cancer Res.* **4**:1193–1201 (1998).
14. M. R. Cooper, R. Lieberman, R. V. La Rocca, P. R. Gernt, M. S. Weinberger, D. J. Headlee, D. R. Kohler, B. R. Goldspiel, C. C. Peck, and C. E. Myers. Adaptive control with feedback strategies for suramin dosing. *Clin. Pharmacol. Ther.* **52**:11–23 (1992).
15. M. A. Eisenberger, V. J. Sinibaldi, L. M. Reyno, R. Sridhara, D. I. Jodrell, E. G. Zuhowski, K. H. Tkaczuk, M. H. Lowitt, R. K. Hemady, and S. C. Jacobs. Phase I and clinical evaluation of a pharmacologically guided regimen of suramin in patients with hormone-refractory prostate cancer. *J. Clin. Oncol.* **13**: 2174–2186 (1995).
16. L. M. Reyno, M. J. Egorin, M. A. Eisenberger, V. J. Sinibaldi, E. G. Zuhowski, and R. Sridhara. Development and validation of a pharmacokinetically based fixed dosing scheme for suramin. *J. Clin. Oncol.* **14**:2187–2195 (1995).
17. K. Kobayashi, E. E. Vokes, N. J. Vogelzang, L. Janisch, B. Soliven, and M. J. Ratain. Phase I study of suramin administered by intermittent infusion without adaptive control to cancer patients: update of two expanded dose levels near the maximally tolerated dose. *J. Clin. Oncol.* **14**:2622–2623 (1996).
18. S. Song, B. Yu, Y. Wei, M. G. Wientjes, and J. L. Au. Low-dose suramin enhanced paclitaxel activity in chemotherapy-naive and paclitaxel-pretreated human breast xenograft tumors. *Clin. Cancer Res.* **10**:6058–6065 (2004).
19. Y. Xin, G. Lyness, D. Chen, S. Song, M. G. Wientjes, and J. L. Au. Low dose suramin as a chemosensitizer of bladder cancer to mitomycin C. *J. Urol.* **174**:322–327 (2005).
20. B. Yu, S.-H. Song, M. G. Wientjes, and J. L. Au. Suramin enhances activity of CPT-11 in human colorectal xenograft tumors. *Proc. Am. Assoc. Cancer Res.* **44**:174 (2003).
21. A. Falcone, E. Pfanner, I. Brunetti, G. Allegrini, M. Lencioni, C. Galli, G. Masi, R. Danesi, A. Antonuzzo, M. Del Tacca, and P. F. Conte. Suramin in combination with 5-fluorouracil (5-FU) and leucovorin (LV) in metastatic colorectal cancer patients resistant to 5-FU+ LV-based chemotherapy. *Tumori* **84**:666–668 (1998).
22. A. Falcone, A. Antonuzzo, R. Danesi, G. Allegrini, L. Monica, E. Pfanner, G. Masi, S. Ricci, M. Del Tacca, and P. F. Conte. Suramin in combination with weekly epirubicin for patients with advanced hormone-refractory prostate carcinoma. *Cancer* **86**: 470–476 (1999).
23. B. L. Rapoport, G. Falkson, J. I. Raats, M. de Wet, B. P. Lotz, and H. C. Potgieter. Suramin in combination with mitomycin C in hormone-resistant prostate cancer. A phase II clinical study. *Ann. Oncol.* **4**:567–573 (1993).
24. M. A. Villalona-Calero, M. G. Wientjes, G. A. Otterson, S. Kanter, D. Young, A. J. Murgo, B. Fischer, C. DeHoff, D. Chen, T. K. Yeh, S. Song, M. Grever, and J. L. Au. Phase I study of low-dose suramin as a chemosensitizer in patients with advanced non-small cell lung cancer. *Clin. Cancer Res.* **9**:3303–3311 (2003).
25. M. Kassack and P. Nickel. Rapid, highly sensitive gradient narrow-bore high-performance liquid chromatographic determination of suramin and its analogues. *J. Chromatogr. B Biomed. Appl.* **686**:275–284 (1996).
26. D. M. Ornitz and N. Itoh. Fibroblast growth factors. *Genome Biol.* **2**:3005 (2001).
27. P. Tothill, L. Matheson, J. Smyth, and K. McKay. Inductively coupled plasma mass spectrometry for the determination of platinum in animal tissues and a comparison with atomic absorption spectrometry. *J. Anal. At. Spectrom.* **5**:619–622 (1990).
28. L. B. Sheiner, B. Rosenberg, and V. V. Marathe. Estimation of population characteristics of pharmacokinetic parameters from routine clinical data. *J. Pharmacokinet. Biopharm.* **5**:445–479 (1977).
29. J. W. Mandema, D. Verotta, and L. B. Sheiner. Building population pharmacokinetic–pharmacodynamic models. I. Models for covariate effects. *J. Pharmacokinet. Biopharm.* **20**:511–528 (1992).
30. W. D. Gabrielsson J. *Pharmacokinetic/Pharmacodynamic Data Analysis: Concepts and Applications*. Swedish Pharmaceutical Press, 1994.
31. A. H. Calvert, D. R. Newell, L. A. Gumbrell, S. O'Reilly, M. Burnell, F. E. Boxall, Z. H. Siddik, I. R. Judson, M. E. Gore, and E. Wiltshaw. Carboplatin dosage: prospective evaluation of a simple formula based on renal function. *J. Clin. Oncol.* **7**: 1748–1756 (1989).
32. M. T. Huizing, A. C. Keung, H. Rosing, V. van der Kuij, W. W. Bokkel Huinink, I. M. Mandjes, A. C. Dubbelman, H. M. Pinedo, and J. H. Beijnen. Pharmacokinetics of paclitaxel and metabolites in a randomized comparative study in platinum-pretreated ovarian cancer patients. *J. Clin. Oncol.* **11**:2127–2135 (1993).
33. M. T. Huizing, L. J. Warmerdamvan, H. Rosing, M. C. Schaefers, A. Lai, T. J. Helmerhorst, C. H. Veenhof, M. J. Birkhofer, S. Rodenhuis, J. H. Beijnen, and W. W. Bokkel Huinink. Phase I and pharmacologic study of the combination paclitaxel and carboplatin as first-line chemotherapy in stage III and IV ovarian cancer. *J. Clin. Oncol.* **15**:1953–1964 (1997).
34. N. Siddiqui, A. V. Boddy, H. D. Thomas, N. P. Bailey, L. Robson, M. J. Lind, and A. H. Calvert. A clinical and pharmacokinetic study of the combination of carboplatin and paclitaxel for epithelial ovarian cancer. *Br. J. Cancer* **75**: 287–294 (1997).
35. P. R. Hoban, M. I. Walton, C. N. Robson, J. Godden, I. J. Stratford, P. Workman, A. L. Harris, and I. D. Hickson. Decreased NADPH: cytochrome P-450 reductase activity and impaired drug activation in a mammalian cell line resistant to mitomycin C under aerobic but not hypoxic conditions. *Cancer Res.* **50**:4692–4697 (1990).
36. H. F. Bligh, A. Bartoszek, C. N. Robson, I. D. Hickson, C. B. Kasper, J. D. Beggs, and C. R. Wolf. Activation of mitomycin C by NADPH:cytochrome P-450 reductase. *Cancer Res.* **50**: 7789–7792 (1990).
37. R. D. Traver, D. Siegel, H. D. Beall, R. M. Phillips, N. W. Gibson, W. A. Franklin, and D. Ross. Characterization of a polymorphism in NAD(P)H: quinone oxidoreductase (DT-diaphorase). *Br. J. Cancer* **75**:69–75 (1997).
38. D. I. Jodrell, L. M. Reyno, R. Sridhara, M. A. Eisenberger, K. H. Tkaczuk, E. G. Zuhowski, V. J. Sinibaldi, M. J. Novak, and M. J. Egorin. Suramin: development of a population pharmacokinetic model and its use with intermittent short infusions to control plasma drug concentration in patients with prostate cancer. *J. Clin. Oncol.* **12**:166–175 (1994).
39. P. R. Hutson, K. D. Tutsch, and G. Wilding. Pharmacokinetic analysis and adaptive control of suramin. In Z. D'Argenio (ed.), *Advanced Methods of Pharmacokinetic and Pharmacodynamic Systems Analysis, Volume 2*, Plenum Press, New York, 1995, pp. 177–187.
40. J. M. Collins, R. W. Klecker Jr., R. Yarchoan, H. C. Lane, A. S. Fauci, R. R. Redfield, S. Broder, and C. E. Myers. Clinical pharmacokinetics of suramin in patients with HTLV-III/LAV infection. *J. Clin. Pharmacol.* **26**:22–26 (1986).
41. S. C. Piscitelli, A. Forrest, R. M. Lush, N. Ryan, L. R. Whitfield, and D. Figg. Pharmacometric analysis of the effect of furosemide on suramin pharmacokinetics. *Pharmacotherapy* **17**: 431–437 (1997).
42. P. R. Hutson, K. D. Tutsch, R. Rago, R. Arzoomanian, D. Alberti, M. Pomplun, D. Church, R. Marnocha, A. L. Cheng, N. Kehrli, and G. Wilding. Renal clearance, tissue distribution, and CA-125 responses in a phase I trial of suramin. *Clin. Cancer Res.* **4**:1429–1436 (1998).
43. W. P. McNally, P. D. DeHart, C. Lathia, and L. R. Whitfield. Distribution of [^{14}C]suramin in tissues of male rats following a single intravenous dose. *Life Sci.* **67**:1847–1857 (2000).